

results confirm the gross aspects of current interpretation of the behavior of a superconducting sphere in the intermediate state. Temperature changes observed on magnetization were in quantitative agreement with

values predicted from calorimetric data and demonstrate a linear relationship between the applied magnetic field and the fraction of normal metal produced in the intermediate state.

## Electrical Properties of Silicon Containing Arsenic and Boron

F. J. MORIN AND J. P. MAITA

*Bell Telephone Laboratories, Murray Hill, New Jersey*

(Received April 28, 1954)

Electrical conductivity and Hall effect have been measured from 10° to 1100° Kelvin on single-crystal silicon containing arsenic and boron. Extrinsic carrier concentration is computed from Hall coefficient. Analysis of extrinsic carrier concentration indicates the ionization energy of arsenic donor levels to be 0.049 ev and of boron acceptor levels to be 0.045 ev for low impurity concentrations. Fermi degeneracy is found to occur in the range  $10^{18}$  to  $10^{19}$  cm<sup>-3</sup> impurity concentration. Extrinsic Hall mobility is computed from Hall coefficient and conductivity. Curves of Hall mobility against resistivity at 300°K are computed from theory and compared with experiment. The temperature dependence of lattice-scattering mobility is found from conductivity to be  $T^{-2.6}$  for electrons and  $T^{-2.3}$  for holes. From conductivity mobility and intrinsic conductivity, it is found that carrier concentration at any temperature below 700°K is given by the expression:  $np = 1.5 \times 10^{23} T^3 \exp(-1.21/kT)$ . The temperature dependence of the ratio Hall mobility/conductivity mobility is determined for holes and electrons.

### 1. INTRODUCTION

AN extensive investigation of the fundamental electrical properties of silicon has not been published since 1949, when Pearson and Bardeen reported on silicon containing boron and phosphorus.<sup>1</sup> Their experimental work was necessarily limited because neither single crystals nor the means for measuring below 77°K were then available. Recently, it seemed opportune to reinvestigate silicon: good quality single crystals were available; it became possible to make the low temperature measurements necessary to locate precisely the impurity levels; there was considerable interest in silicon and fundamental information was needed.

Electrical conductivity and Hall effect have been measured from 10° to 1100°K on single crystals of silicon containing arsenic and boron. Unfortunately a complete analysis of the data is not possible at present. For example, one needs to know more about the scattering processes which produce the departure from the  $T^{-1.5}$  law of lattice scattering mobility found for both holes and electrons; it is shown that electron-hole scattering is probably negligible below 1200°K; only a very rough estimate of optical mode scattering can be made; the possibility of scattering by multiple constant energy surfaces and by band splitting due to spin-orbit coupling was suggested by C. Herring but is neglected because theory is lacking. The meaning of the low temperature Hall effect in some samples is uncertain. Behavior of computed Hall mobility suggests the presence of impurity level conduction for which theory

is unavailable. Determination of the mass parameter by fitting carrier concentration data in the extrinsic range is faced with two new problems for which theory is unavailable: the apparent dependence of the mass parameter on impurity concentration and the possible existence of excited states associated with the impurity atoms.

#### 1.1 Methods

Crystals were prepared by E. Shannon of these laboratories using the Teal-Little pull technique.<sup>2</sup> In each case two crystals were pulled from du Pont silicon and then combined with the added impurity in a melt from which the final crystal was pulled. Samples were bridge shape<sup>3</sup> cut with the [110] direction along the length of the sample. The samples were sandblasted. Contact was made to *n*-type samples by bonding through gold plate with Sb-doped gold wire. Contacts to *p*-type samples were pressure contacts on rhodium plate.

#### 1.2 Symbols

The symbols used have been defined previously by the authors.<sup>4</sup>

### 2. EXPERIMENTAL RESULTS

Conductivity and Hall coefficient in the intrinsic range of silicon are shown in Fig. 1. The Hall coefficient

<sup>2</sup> G. K. Teal, Phys. Rev. **78**, 647 (1950); Teal, Sparks, and Buehler, Phys. Rev. **81**, 637 (1951).

<sup>3</sup> P. Debye and E. Conwell, Phys. Rev. **93**, 693-706 (1954).

<sup>4</sup> F. J. Morin and J. P. Maita, Phys. Rev. **94**, 1525 (1954). See Sec. 3 for definition of symbols.

<sup>1</sup> G. L. Pearson and J. Bardeen, Phys. Rev. **75**, 865-883 (1949).

is negative, indicating that electron mobility is greater than hole mobility. The rapid downward curvature of the Hall coefficient suggests that electron and hole mobilities are converging at high temperature. Conductivity from  $\sim 400^\circ$  to  $600^\circ\text{K}$  is a combination of intrinsic and extrinsic. At high temperature, conductivity is intrinsic and follows a straight line. This is in contrast to the curvature found in the intrinsic range of germanium and attributed to electron-hole scattering.<sup>4</sup> Extrinsic conductivity and Hall coefficient in silicon containing arsenic are shown in Figs. 2 and 4 and in silicon containing boron in Figs. 3 and 5. The sign of the Hall effect indicates arsenic to be a donor and boron to be an acceptor. The curves are displaced in the expected way by the change in amount of added impurity. Sample 159 represents the control to which no impurity was intentionally added. Samples 140 and 125 contain the highest concentration of impurity and show Fermi degeneracy. In the temperature range  $10^\circ$ – $100^\circ\text{K}$  the remaining curves have slopes indicating ionization of impurity centers with increasing temperature. Near  $300^\circ$  impurity centers are almost completely ionized and carrier concentration is constant. In this range conductivity changes with the temperature variation of mobility, and Hall coefficient changes with the temperature variation of the ratio  $\mu_H/\mu_e$ . Samples 126 and 141 depart at low temperature from the behavior common to the other nondegenerate samples. This result is not understood. It is shown later to include anomalous behavior of computed carrier concentration and Hall mobility.

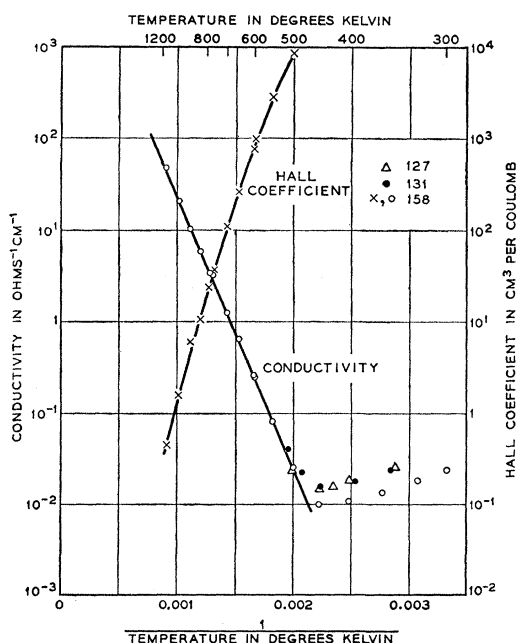


Fig. 1. Conductivity and Hall coefficient in the intrinsic range of silicon as a function of reciprocal absolute temperature.

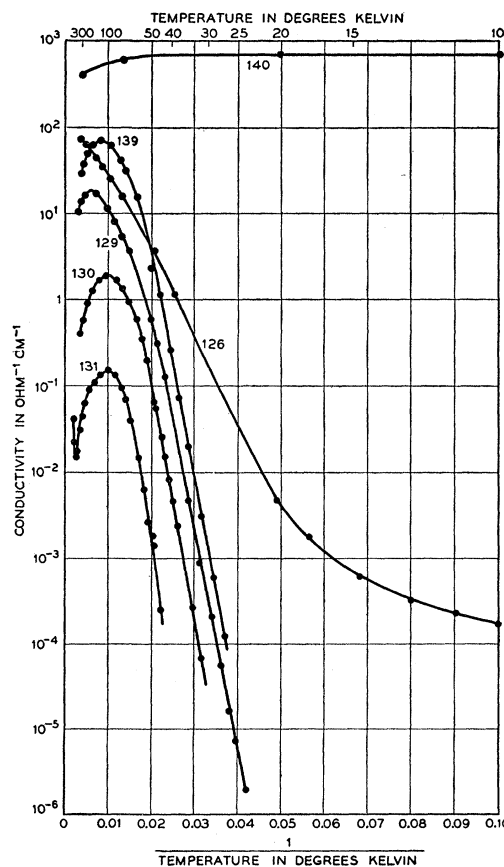


Fig. 2. Conductivity of silicon samples containing arsenic as a function of reciprocal absolute temperature. Composition of samples given in Table I.

### 3. EXTRINSIC RANGE

It is the plan of this paper to consider first the extrinsic range data and then to use some of the results obtained to analyze the intrinsic range. Carrier concentration and Hall mobility are computed from extrinsic conductivity and Hall coefficient. The concentration and ionization energies of impurities and the mass parameters for holes and electrons are determined from carrier concentration results. Curves of Hall mobility as a function of resistivity at  $300^\circ\text{K}$  are computed from theory, assuming lattice scattering and ionized impurity scattering and using the impurity concentrations determined from the carrier concentration analysis. This serves as a rough check on the impurity concentrations as determined, and on the general perfection of the samples.

#### 3.1 Carrier Concentration

Carrier concentration has been computed from the Hall coefficient using the relations

$$R_H = 3/8en \quad (\text{or } p) \quad (\text{impurity range}),$$

$$R_H = 1/en \quad (\text{or } p) \quad (\text{degenerate range}),$$

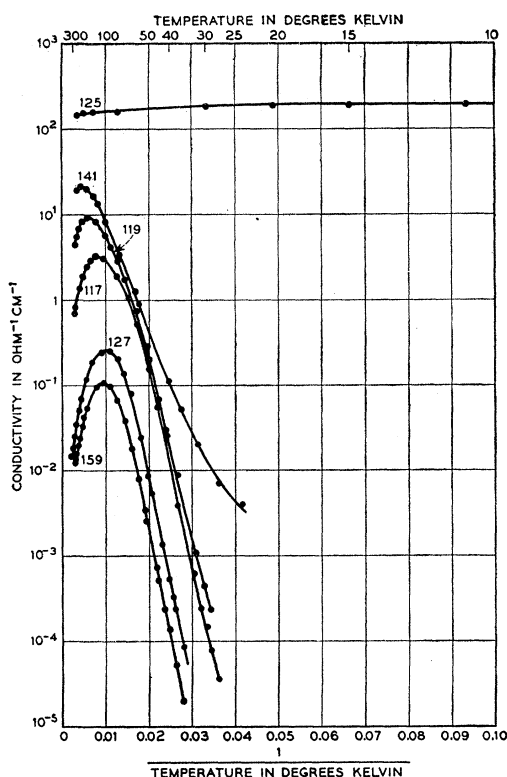


FIG. 3. Conductivity of silicon samples containing boron as a function of reciprocal absolute temperature. Composition of samples given in Table I.

and is shown in Fig. 6 for electrons and Fig. 7 for holes. The solid lines have been computed to fit the data by a method similar to that described in reference 1. The values found by this computation for concentrations and ionization energies of impurities and for the mass parameters of electrons and holes are shown in Table I. The ionization energy of arsenic levels appears to be 0.049 ev and of boron levels 0.045 ev under condition of high dilution of the impurities. These values are about the same as those found by Pearson and Bardeen,  $\sim 0.046$  ev, for both donors (phosphorus) and acceptors

TABLE I. Composition of samples and summary of extrinsic range results.

Sample No.	Majority impurity ionization energy ev	Net impurity concentration $\text{cm}^{-3}$	Minority impurity concentration $\text{cm}^{-3}$	Mass parameter	Added impurity
<i>n</i> type					
131	0.056	$1.75 \times 10^{14}$	$1.0 \times 10^{14}$	0.5	arsenic
130	0.049	$2.1 \times 10^{15}$	$5.25 \times 10^{14}$	1.0	arsenic
129	0.048	$1.75 \times 10^{16}$	$1.48 \times 10^{15}$	1.2	arsenic
139	0.046	$1.3 \times 10^{17}$	$2.2 \times 10^{15}$	1.0	arsenic
126	?	$2.2 \times 10^{18}$	...	...	arsenic
140	degenerate	$2.7 \times 10^{19}$	...	...	arsenic
<i>p</i> type					
159	0.045	$3.1 \times 10^{14}$	$4.1 \times 10^{14}$	0.4	none
127	0.045	$7.0 \times 10^{14}$	$2.2 \times 10^{14}$	0.4	boron
117	0.043	$2.4 \times 10^{16}$	$2.3 \times 10^{15}$	0.6	boron
119	0.043	$2.0 \times 10^{17}$	$4.9 \times 10^{15}$	0.7	boron
141	?	$1 \times 10^{18}$	...	...	boron
125	degenerate	$1.5 \times 10^{19}$	...	...	boron

(boron) if their sample 1 results are neglected on the grounds (suggested by its behavior) that the sample probably contained *n-p* junctions. The value of 0.056 ev for sample 131 seems out of line and the following possible explanation is given for this result. Crystals grown from undoped silicon are *p* type. In preparing 131, an amount of arsenic (donor) was added which together with the unknown donors normally present, compensated the acceptors and produced an *n*-type sample. Compensation may have been sufficient to ionize all of the arsenic (0.049 ev levels) plus some of the unknown donor (0.056 ev levels) with the consequence that the 0.049 ev levels were undetected by the Hall effect measurement. It is possible, therefore, that there is a higher concentration of impurities in sample 131 than shown in Table I. As shown by the mobility analysis in Sec. 3.2, the concentration of impurities may be as high as  $2 \times 10^{15} \text{ cm}^{-3}$ .

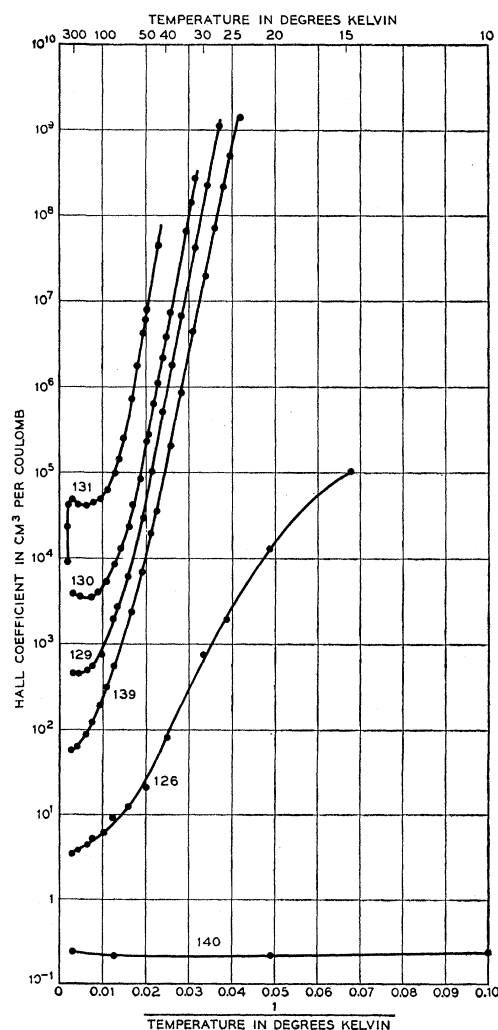


FIG. 4. Hall coefficient of silicon samples containing arsenic as a function of reciprocal absolute temperature. Composition of samples given in Table I.

It is not clear from the analysis of carrier concentrations how impurity ionization energy varies with impurity concentration. The effect is obscured by some new process occurring at low temperatures and superimposed upon the normal impurity ionization process. This can be seen as curvature in the low temperature carrier concentration results for samples 126 and 141. Evidence that this is not due to transition into Fermi degeneracy is given by their apparent Hall mobility which at low temperature drops well below that of the degenerate samples. Fermi degeneracy occurs at an impurity concentration between  $10^{18}$  and  $10^{19}$   $\text{cm}^{-3}$ . It occurs in germanium at about one decade less in impurity concentration.

The analysis of carrier concentration does not give a very useful value for the inertial mass of the carriers. As shown in Table I, the mass parameter is found to vary with impurity concentration. Theory has not been developed for such a dependence. It is also probable that impurity levels have excited states. These cause the carrier concentration and, therefore, the

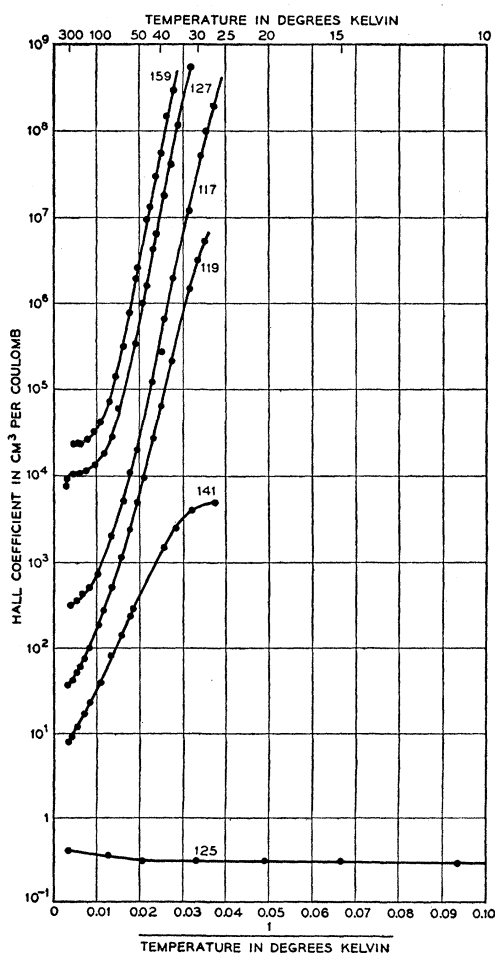


FIG. 5. Hall coefficient of silicon samples containing boron as a function of reciprocal absolute temperature. Composition of samples given in Table I.

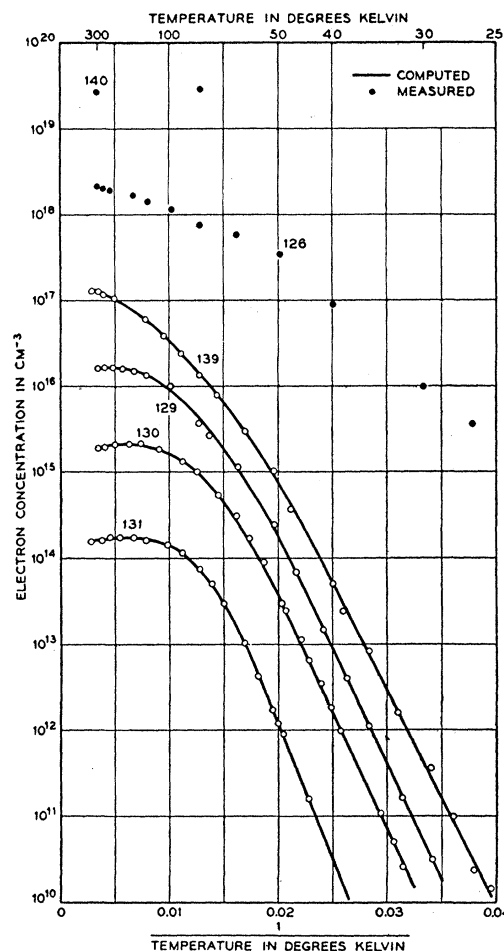


FIG. 6. Charge carrier concentration in silicon samples containing arsenic as a function of reciprocal absolute temperature.

computed mass parameter to be less than that predicted by the simple theory which assumes only a ground state.

### 3.2 Hall Mobility

Hall mobility, the product of conductivity and Hall coefficient, is shown in Figs. 8 for electrons and 9 for holes. The low temperature behavior of samples 139, 126, 119, and 141 is anomalous. No ordinary scattering mechanism predicts the rapid drop in mobility with decreasing temperature found in these samples. This result suggests the presence of a different conduction process, probably impurity level conduction, occurring at low temperatures and with low mobility carriers.

Hall mobility as a function of resistivity, both taken at 300°K, is shown in Figs. 10 and 11. The solid lines were computed by combining<sup>5</sup> lattice scattering and ionized impurity scattering mobilities. This computation was intended as a rough check on the impurity concentrations determined from carrier concentration. In making the computation it was assumed that

<sup>5</sup> Using the method of Conwell in reference 3.

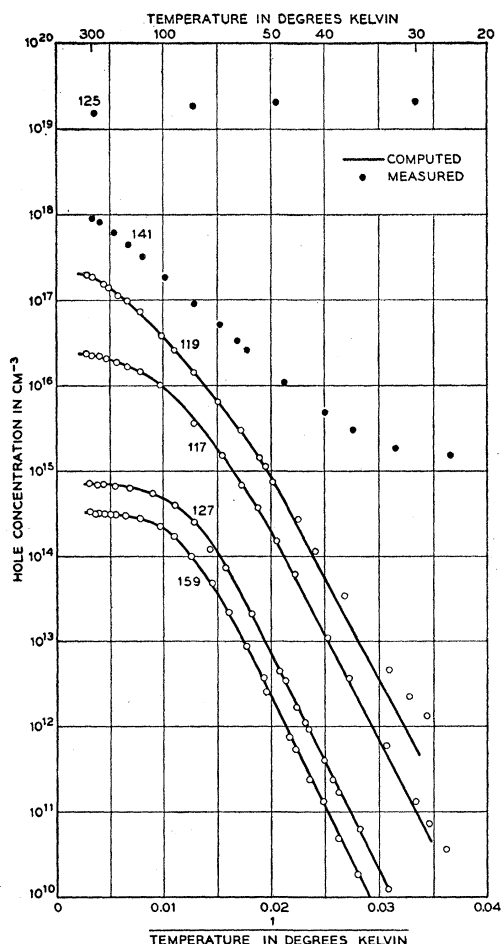


FIG. 7. Charge carrier concentration in silicon samples containing boron as a function of reciprocal absolute temperature.

$\mu_H/\mu_c = 1.0$  and is constant with impurity concentration. Lattice scattering mobility was used as an adjustable parameter to move the curve along the mobility axis and give the best fit to measured values. For the computation lattice scattering mobility was taken to be  $1700 \text{ cm}^2/\text{volt sec}$  for electrons and  $350 \text{ cm}^2/\text{volt sec}$  for holes. Ionized impurity scattering was computed using the modified Conwell-Weisskopf formula<sup>3</sup> and the impurity concentrations determined in Sec. 3.1. The resulting fit to the data suggests that the ionized impurities observed by the Hall effect make up the majority of scattering centers in the samples investigated. Sample 131 is the exception. Its mobility lies below the computed value by a significant amount. It is consistent with the carrier concentration results described in Sec. 3.1 to assume the low mobility to be due to ionized impurity scattering. The observed lowering of lattice scattering mobility requires a concentration of  $2 \times 10^{15} \text{ cm}^{-3}$  ionized impurities, about seven times the amount detected by the Hall effect.

#### 4. INTRINSIC RANGE

In this section intrinsic carrier concentration is computed from conductivity and conductivity mobility. From these results an empirical expression for the temperature dependence of carrier concentration is obtained. An estimate is made of the temperature behavior of  $\mu_H/\mu_c$  necessary to bring carrier concentration from Hall coefficient into agreement with that determined from conductivity.

##### 4.1 Lattice Scattering Mobility

Conductivity mobility has been determined by the method described by Morin<sup>6</sup> using the conductivity of *n*-type samples 130 and 131 and *p*-type samples 127 and 159, together with drift mobilities at  $300^\circ\text{K}$  measured by Prince<sup>7</sup> ( $1300 \text{ cm}^2/\text{volt sec}$  for electrons and  $500 \text{ cm}^2/\text{volt sec}$  for holes). The results are shown as plotted points in Fig. 12. Using the impurity concentrations determined in Sec. 3.1 it can be shown that impurity scattering in samples 127 and 159 is negligible above  $150^\circ\text{K}$  and that the results in Fig. 12 for holes represent lattice scattering mobility. This is not true

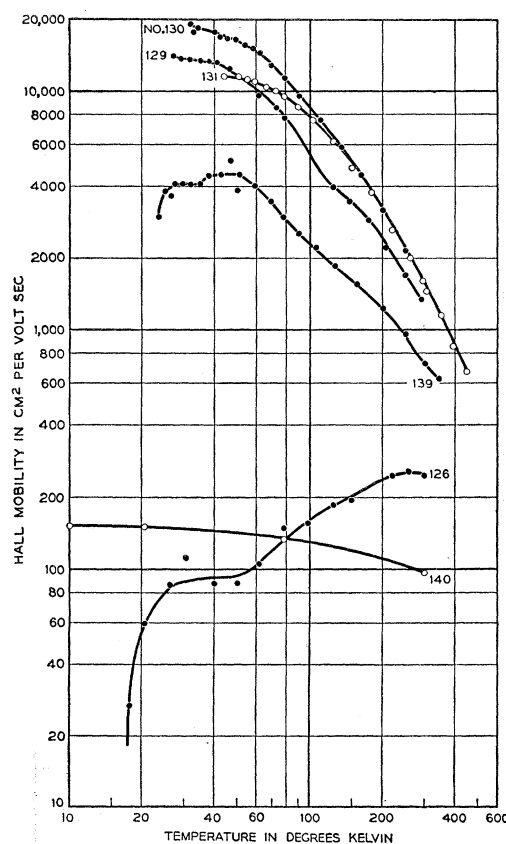


FIG. 8. Hall mobility of electrons in silicon samples containing arsenic as a function of absolute temperature.

<sup>6</sup> F. J. Morin, Phys. Rev. **93**, 62-63 (1954).

<sup>7</sup> M. Prince, Phys. Rev. **93**, 1204-1206 (1954).

for the electron results which must be corrected for impurity scattering. Electron lattice scattering mobility has been determined from measured mobility and computed ionized impurity scattering mobility. For this computation ionized impurity concentration was assumed to be  $2.6 \times 10^{15} \text{ cm}^{-3}$ , that found in Sec. 3.1 for sample 130 and which is also a reasonable value for sample 131. The results are given by the relations

$$\mu_{Ln} = 4.0 \times 10^9 T^{-2.6}, \quad (1)$$

$$\mu_{Lp} = 2.5 \times 10^8 T^{-2.3}, \quad (2)$$

and shown by the straight lines in Fig. 12. The temperature dependence of  $\mu_L$  departs from the  $T^{-1.5}$  law expected for acoustical mode scattering. According to Herring, these results may be due to optical mode scattering, to the band edges being located at some point other than the center of the Brillouin zone, to bands split by spin-orbit coupling, or to a combination of these effects.

A computation has been made to find out what effect the presence of optical modes might have on an extrapolation of  $\mu_L$  to higher temperatures. The optical mode temperature  $\theta$  for silicon has been computed by Herring to be  $\sim 1200^\circ\text{K}$ , using optical mode frequency

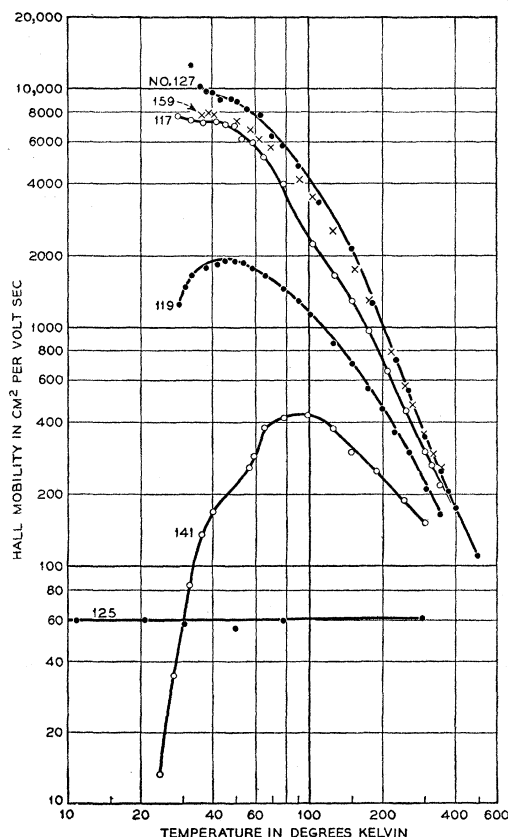


Fig. 9. Hall mobility of holes in silicon samples containing boron as a function of absolute temperature.

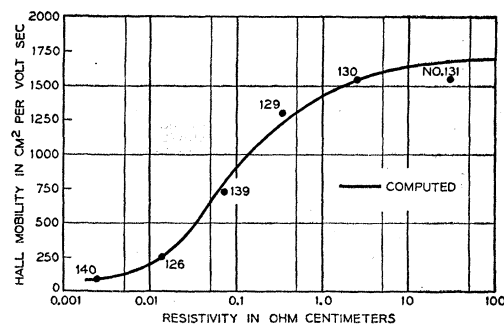


Fig. 10. Hall mobility of electrons as a function of resistivity in silicon samples containing arsenic.

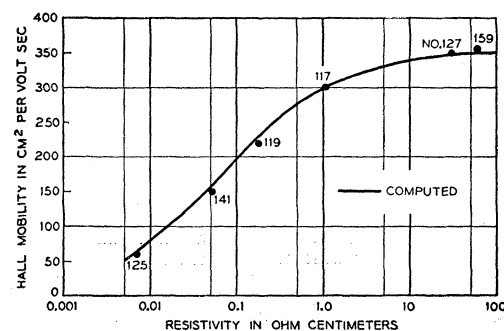


Fig. 11. Hall mobility of holes as a function of resistivity in silicon samples containing boron.

results of Smith.<sup>8</sup> From this result and Eq. (2), reference 4, the optical mode temperature dependence has been computed and is shown in Fig. 12. It is evident that if optical modes make an appreciable contribution to scattering at high temperatures (as they are expected to) they will also contribute appreciably to the scattering in the range where  $\mu_L$  has been measured. A computation similar to that described in Sec. 4.1, reference 4, indicates that a large part (but probably not all) of the departure of the mobility temperature dependence from the  $T^{-1.5}$  law might be due to optical modes. However, the results indicate that a large optical mode contribution does not cause the lattice scattering mobility to depart importantly from the linear extrapolation shown in Fig. 12.

#### 4.2 Electron-Hole Scattering

Electron hole scattering has been computed using the equation in Sec. 5.1 of reference 4 with  $m_n = m_p = m$  and  $\kappa = 12$ . Results are shown in Fig. 12. The effect of electron-hole scattering on mobility is negligible below  $1200^\circ\text{K}$ .

#### 4.3 Carrier Concentration

Carrier concentration in the intrinsic range has been computed from conductivity and from mobility given

<sup>8</sup> H. M. J. Smith, Trans. Roy. Soc. (London) 241, 105 (1948-1949).

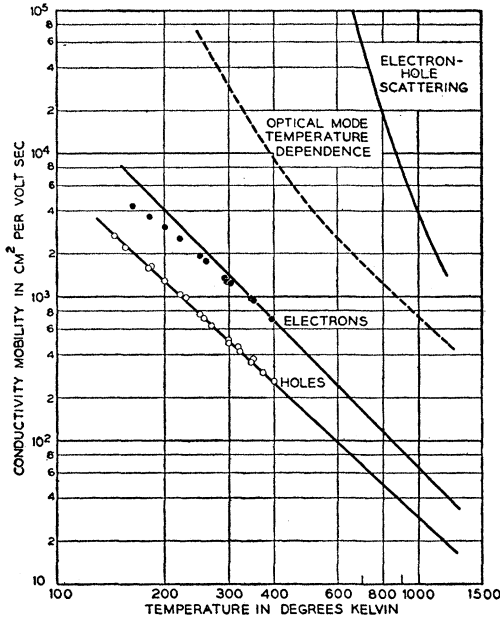


FIG. 12. Conductivity mobility as a function of absolute temperature.

by Eqs. (1) and (2). The method of computation used in the region of mixed intrinsic and extrinsic conductivity has been described in reference 4, Sec. 4.2. Results are shown in Fig. 13 as plotted points. From these the following empirical expression has been derived:

$$np = 1.5 \times 10^{23} T^3 \exp(-1.21/Tk), \quad (3)$$

which fits the measured points below 700°K. Above this temperature the width of the forbidden region

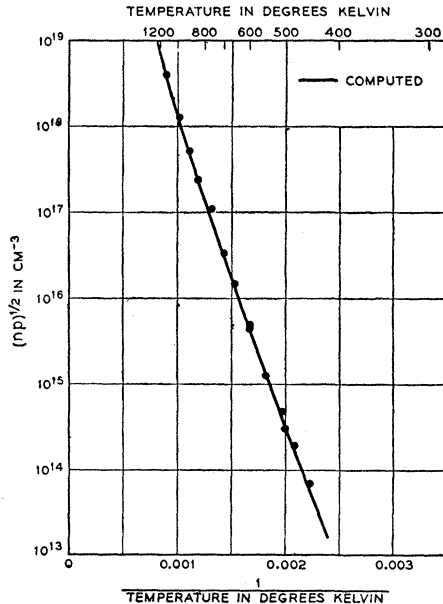


FIG. 13. Carrier concentration in the intrinsic range of silicon as a function of reciprocal absolute temperature.

depends appreciably upon the electrostatic interaction of charge carriers. The effect of this dependence on  $np$  has been determined as described in reference 4, Sec. 5.2, using the relation

$$\Delta E_G = -7.1 \times 10^{-10} (np)^{1/2} T^{-1/2}. \quad (4)$$

From Eqs. (3) and (4) the solid line shown in Fig. 13 has been computed. The value of  $(np)^{1/2}$  at 1000°K computed from Eqs. (3) and (4) is 13 percent greater than  $(np)^{1/2}$  computed from Eq. (3) alone.

From lattice scattering conductivity mobility of Fig. 12 and  $(np)^{1/2}$  from Eq. (3), intrinsic resistivity of silicon is found to be  $2.3 \times 10^5$  ohm cm at 300°K.

#### 4.4 Temperature Dependence of $E_G$

The theoretical formula for carrier concentration in the intrinsic range, Eq. (16), reference 4, has the same form as empirical equation (3) but the numerical factor in (3) is larger than the theoretical value by a factor

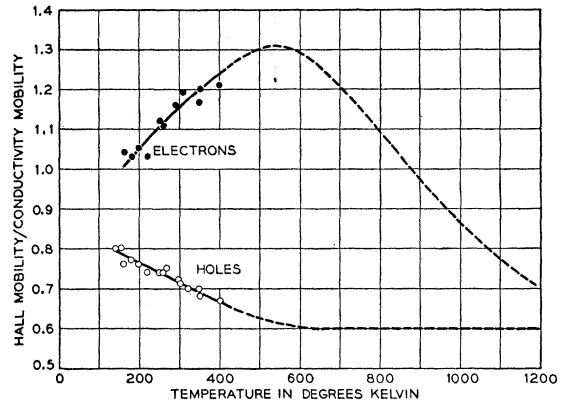


FIG. 14. Hall mobility/conductivity mobility as a function of absolute temperature for electrons and holes in silicon.

of 63. Assuming  $m_n = m_p = m$ , and taking the discrepancy in the numerical factor to be due to a linear variation of  $E_G$  with temperature, leads to a temperature coefficient for  $E_G$  of  $3.6 \times 10^{-4}$  ev/degree.  $E_G(T=0)$  found in section 4.3 is 1.21 ev. These values are somewhat higher than the corresponding  $3.0 \times 10^{-4}$  ev/degree and 1.12 ev found by Pearson and Bardeen,<sup>1</sup> who assumed the temperature dependence of mobility to be  $T^{-1.5}$ .

#### 4.5 Hall Coefficient and $\mu_H/\mu_c$

Hall coefficient is given by Eq. (15), reference 4. All of the parameters in that equation have been determined except  $\mu_{Hn}/\mu_{cn}$  and  $\mu_{Hp}/\mu_{cp}$ . In this section a possible temperature dependence for these two parameters is discussed.

$\mu_H/\mu_c$  for electrons and holes has been computed from measured  $\mu_H$  and  $\mu_c$  for samples 130, 131, 127, and 159 and is shown as plotted points in Fig. 14. It was

assumed that the  $\mu_{Hp}/\mu_{cp}$  temperature dependence is given by the dotted line for holes in Fig. 14. With this extrapolation and the carrier concentration and mobility results of the preceding sections, the Hall coefficient relation was used to compute  $\mu_{Hn}/\mu_{cn}$ . This result is shown by the dotted line for electrons in Fig. 14. According to Herring these results are what one would expect if the conduction band were composed of multiple surfaces of minimum energy, and the valence band of some structure other than a spherical energy surface. However, on this basis,  $\mu_{Hp}/\mu_{cp}$  is lower than the expected  $\mu_H/\mu_c > 1$ . A similar result was found at one time for electrons in germanium.<sup>9</sup> This discrepancy dis-

appeared as improved germanium crystals were made. Presumably this same effect may be lowering the  $\mu_H/\mu_c$  values found for both electrons and holes in silicon.<sup>10</sup> It is assumed that, with improvement of the material,  $\mu_{Hp}/\mu_{cp}$  will approach  $\sim 1$ , then the peak value for  $\mu_{Hn}/\mu_{cn}$  increasing proportionally may approach  $\sim 2.2$ . This is reasonable in the light of the germanium results<sup>6</sup> where the highest value measured was  $\mu_{Hp}/\mu_{cp} \sim 1.8$ .

#### ACKNOWLEDGMENT

The authors wish to thank C. Herring for his considerable assistance in interpreting the data.

<sup>9</sup> W. Shockley, *Electrons and Holes in Semiconductors* (D. Van Nostrand Company, Inc., New York, 1950), first edition, p. 338.

<sup>10</sup> Note added in proof.—See the more recent Hall mobility results of P. P. Debye and T. Kohane, *Phys. Rev.* **94**, 724 (1954).

## Secondary Electron Yield from Al by High-Energy Primary Electrons\*

G. W. TAUTFEST AND H. R. FECHTER†

*W. W. Hansen Laboratories of Physics, Stanford University, Stanford, California*

(Received June 3, 1954)

The yield of secondary electrons from thin (1.71 mg/cm<sup>2</sup>) aluminum foils by high-energy primary electrons is reported. The value is  $0.0397 \pm 0.0003$  secondary electron per primary electron from both sides of the foil. The result is independent of the primary-electron energy in the range 111–235 Mev.

IN connection with the development of a non-saturable monitor<sup>1</sup> for electron beams, we have measured the yield of secondary electrons from thin (1.71 mg/cm<sup>2</sup>) aluminum foils under bombardment by 150-Mev electrons. A general diagram of the experimental arrangement is shown in Fig. 1.

A monoenergetic beam of electrons from the Stanford Mark III linear accelerator is stripped to  $\frac{1}{16}$ -inch diameter by a uranium collimator, and, after passing through the double-deflection system<sup>2</sup> of the linear accelerator at the 130-ft station, is brought to a focus on a set of twenty aluminum foils, each  $2\frac{1}{2}$  inches by 4 inches in size and 0.00025 inch thick. Alternate foils are connected together and mounted in a vacuum ( $10^{-6}$  mm Hg) on polystyrene insulators. One set of foils is biased to a negative potential of 1 kv with respect to the second set which is connected via a vacuum feed-through to a grounded condenser. After passing through the foils, the beam is collected in a lead Faraday-cup integrator. The ratio of the charge in-

tegrated on the condenser to the charge collected in the Faraday cup when averaged over the ten foils gives directly the number of secondary electrons liberated from both sides of the foil by a primary electron. The ratio we obtain is  $0.0397 \pm 0.0003$  secondary electron per primary electron, which is in qualitative agreement with low-energy experimental data.<sup>3</sup> No theory of secondary-electron yields at these energies exists.

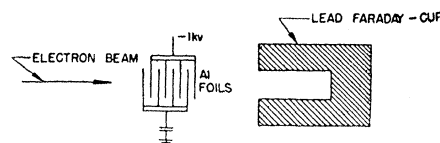


FIG. 1.

Since the theoretical energy distribution of secondary electrons with kinetic energy  $W > 2$  kev varies as  $1/W^2$ , the high-energy secondaries which are not collected in our arrangement give negligible correction to the above ratio. The ratio was found to be independent of the bias voltage from 300 volts to 2 kv and to be independent of the primary-electron energy in the range 111–235 Mev.

<sup>3</sup> Shatas, Marshall, and Pomerantz, *Phys. Rev.* **94**, 757 (1954).

\* The research reported in this document was supported jointly by the U. S. Office of Naval Research and the U. S. Atomic Energy Commission.

† Now at the Stanford Research Institute, Stanford, California.

<sup>1</sup> G. W. Tautfest and H. R. Fechter, *Rev. Sci. Instr.* (to be published).

<sup>2</sup> W. K. H. Panofsky and J. A. McIntyre, *Rev. Sci. Instr.* **25**, 287 (1954).